Journal of Solid State Chemistry **165,** 94–99 (2002)
doi:10.1006/jssc.2001.9503, available online at http://www/idealibrary.com on IDEAL®

$FeGa_3$ and $RuGa_3$: Semiconducting Intermetallic Compounds

Ulrich Häussermann,*[,1] Magnus Boström,† Per Viklund,‡ Östen Rapp,§ and Therese Björnängen§

*Department of Inorganic Chemistry, Stockholm University, S-10691 Stockholm, Sweden; †Department of Structural Chemistry, Stockholm University, S-10691 Stockholm, Sweden; ‡Department of Inorganic Chemistry 2, Lund University, S-22100 Lund, Sweden; and §Department of Solid State Physics, Royal Institute of Technology, S-10044 Stockholm, Sweden

Received September 18, 2001; in revised form December 26, 2001; accepted January 4, 2002

The intermetallic compounds $FeGa_3$ and $RuGa_3$ were prepared from the elements using a Ga flux and their structures were refined from single-crystal X-ray data. Both compounds crystallize with the $FeGa_3$ structure type (tetragonal, space group $P4_2/mnm$, $Z=4$). Electrical resistivity measurements revealed a semiconducting behavior for $FeGa_3$ and $RuGa_3$, which is in contrast to the good metallic conductivity observed for the isotypic compound $CoGa_3$. The origin of the different electronic properties of these materials was investigated by first-principle calculations. It was found that in compounds adopting the $FeGa_3$ structure type the transition metal atoms and Ga atoms interact strongly. This opens a *d–p* hybridization bandgap with a size of about 0.31 eV in the density of states at the Fermi level for 17-electron compounds (i.e., $FeGa_3$ and $RuGa_3$). The electronic structure of $CoGa_3$ (an 18-electron compound) displays rigid band behavior with respect to $FeGa_3$. As a consequence, the Fermi level in $CoGa_3$ becomes located above the *d–p* hybridization gap which explains its metallic conductivity.

1. INTRODUCTION

Intermetallic compounds formed by elemental metals with good conductivity are usually metallic conductors as well. However, $RuAl_2$ (1, 2) and $RuGa_2$ (3) are reported to be semiconductors. Both compounds crystallize with the $TiSi_2$ structure type and it was suggested by Jeitschko that indeed any 14-electron compound with this structure type should exhibit semiconductivity (4). Recent electronic structure calculations could verify the existence of a bandgap in $RuAl_2$ and $RuGa_2$ which emerges as a result of strong interaction between Ru *d* states and Al(Ga) *p* states (5). In this article we report on the synthesis, structural reinvestigation, and semiconductivity of $FeGa_3$ and $RuGa_3$. By that we enlarge the small and peculiar group of narrow-bandgap semiconductors exclusively composed of good metallic conducting elements to include 17-electron compounds with the composition AB_3.

[1]To whom correspondence should be addressed. Fax: +46-8-152187. E-mail: ulrich@inorg.su.se.

2. EXPERIMENTAL

2.1. Synthesis

The compounds $FeGa_3$ and $RuGa_3$ were prepared from mixtures of the pure elements (Fe powder (ABCR, >99.99%), Ru powder (ABCR, >99.99%), and Ga rod (ABCR, >99.9999%) with a molar *T* (Fe, Ru): Ga ratio of 1:10, thus employing Ga as both reactant and flux medium. The reactants were carefully mixed, pressed into pellets, and loaded into quartz ampoules, which were sealed under vacuum (approx 10^{-4} atm). All samples were heated to 800°C at 200°C/h, held at this temperature for 24 h, and finally cooled to room temperature at the rate of 20°C/h. Excess Ga metal was dissolved with 3 M HCl and the remains were washed with deionized water. The products consisting of well-shaped, silvery-gray, crystals (with sizes up to 1 mm) were characterized by Guinier powder diagrams. Diffractograms were recorded at room temperature with a Huber Guinier G670 image foil powder camera using monochromatized Cu$K\alpha$ radiation with silicon (SICOMILL, Kema Nord, Nobel Industries, Sweden) as internal standard. The products were single phase and all lines of the powder patterns could be indexed with a tetragonal unit cell. Lattice parameters were obtained from least-squares refinements of the measured and indexed lines (program PIRUM (6)).

2.2. Structure Determination

Since $FeGa_3$ and $RuGa_3$ have only been structurally characterized from X-ray powder film investigations several decades ago (7, 8) we performed refinements of single-crystal X-ray diffraction data to obtain precise atomic position parameters. Intensity data were collected from $FeGa_3$ and $RuGa_3$ single crystals on a Siemens

0022-4596/02 $35.00

TABLE 1
X-Ray Single-Crystal Refinement Data for $FeGa_3$ and $RuGa_3$

Parameter	$FeGa_3$	$RuGa_3$
M_w	265.01	310.23
Crystal system	Tetragonal	Tetragonal
Space group	$P4_2/mnm$	$P4_2/mnm$
Personal symbol	$tP16$	$tP16$
a (Å)	6.2628(3)	6.4729(3)
c (Å)	6.5546(5)	6.7062(6)
V (Å^3)	257.09(4)	280.98(3)
Z	4	4
ρ_{calcd} (g cm^{-1})	6.847	7.334
Crystal size (μm^3)	$40\times40\times100$	$45\times45\times80$
Transmission (max:min)	3.34	2.16
μ (mm^{-1})	36.236	33.369
2θ range hkl	9.0–63.4	8.8–51.8
Index range hkl	$-9\le h\le9$	$-7\le h\le7$
	$-9\le k\le8$	$-7\le k\le7$
	$-9\le l\le8$	$-8\le l\le8$
Total No. reflections	2965	1985
R_{int}	0.0626	0.0483
Independent reflections	253	167
Reflections with $I>2\sigma(I)$	202	155
Final R indices [$I>2\sigma(I)$]	$R=0.0336$	$R=0.0322$
	$wR=0.0803$	$wR=0.0902$
R indices (all data)	$R=0.0404$	$R=0.0339$
	$wR=0.0823$	$wR=0.0922$
Extinction coefficient	0.27(1)	0.055(6)
Largest diff. Peak/hole (e Å^{-3})	1.754/−2.104	1.111/−1.673

Note. The lattice parameters were obtained from X-ray powder data. [a] $R_1=\sum||F_o|-|F_c||/\sum|F_o|$. $wR_2=(\sum[w(F_o^2-F_c^2)^2])/(\sum[w(F_o^2)^2])$. $w=1/[\sigma^2(F_o^2)+(aP)^2+bP]$ and $P=(F_o^2+2F_c^2)/3$. $FeGa_3$ ($a=0.0560$, $b=0.00$) $RuGa_3$ ($a=0.0629$, $b=1.80$).

SMART CCD system (9) at room temperature with monochromatized Mo$K\alpha$ radiation (0.71073 Å). The data collection nominally covered a full sphere of reciprocal space. In each case data were corrected for Lorentzian polarization (10), extinction, and absorption (assuming a spherical crystal) (11). The centrosymmetric space group $P4_2/mnm$ was assigned on the basis of the systematic absences and the statistical analysis of the intensity distributions. Both structures were refined against F^2 with the program SHELXTL (12) using the atomic position parameters of $FeGa_3$ obtained by Lu and Ching-Kwei from X-ray powder data (7). Some details of the single-crystal data collections and refinements are listed in Table 1. Atomic position parameters and selected interatomic distances are given in Tables 2–4. Further details of the crystal structure investigation may be obtained from Fachinformationszentrum Karlsruhe, D-76344 Eggenstein-Leopoldshafen, Germany (fax: (+49)7247-808-666; e-mail: crysdata@fiz-karlsruhe.de) on quoting Depository Nos. CSD-412077 ($FeGa_3$) and CSD-412078 ($RuGa_3$).

TABLE 2
Atomic Position Parameters, Site Occupancies, and Isotropic Thermal Displacement Parameters for $FeGa_3$

Atom	$P4_2/mnm$	x	y	z	s.o.f.	U_{eq}
Fe	4f	0.3437(1)	0.3437(1)	0	1	50(4)
Ga1	4c	0	0.5	0	1	103(4)
Ga2	8j	0.1556(1)	0.1556(1)	0.2620(1)	1	89(3)

Note. U_{eq} ($\times10^4$ Å^2) is defined as one-third of the trace of the orthogonalized U_{ij} tensor.

TABLE 3
Atomic Position Parameters, Site Occupancies, and Isotropic Thermal Displacement Parameters for $RuGa_3$

Atom	$P4_2/mnm$	x	y	z	s.o.f.	U_{eq}
Ru	4f	0.3410(1)	0.3410(1)	0	1	180(6)
Ga1	4c	0	0.5	0	1	244(7)
Ga2	8j	0.1547(1)	0.1547(1)	0.2640(1)	1	219(6)

Note. U_{eq} ($\times10^4$ Å^2) is defined as one-third of the trace of the orthogonalized U_{ij} tensor.

2.3. Resistivity Measurement

Resistivity measurements were performed on millimeter-sized single crystals TGa$_3$ (T = Fe, Ru, Co) using a four-point in-line contract arrangement. (Concerning the synthesis of $CoGa_3$ single crystals, se our work (13).) Contacts were prepared by applying strips of liquid silver paint (Demetron D200), which were dried in air. The samples were cooled to about 10 K and then slowly heated to room temperature. During heating, resistances were

TABLE 4
Interatomic Distances (in Å) Calculated with the Lattice Parameters Obtained from X-ray Powder Data of $FeGa_3$ and $RuGa_3$

$FeGa_3$				$RuGa_3$			
Fe:	2	Ga1	2.365	Ru:	2	Ga1	2.435
	2	Ga2	2.393		2	Ga2	2.459
	4	Ga2	2.500		4	Ga2	2.574
	1	Fe	2.769		1	Ru	2.911
Ga1:	2	Fe	2.365	Ga1:	2	Ru	2.435
	4	Ga2	2.835		4	Ga2	2.916
	4	Ga2	2.924		4	Ga2	3.022
	2	Ga1	3.277		2	Ga1	3.353
Ga2:	1	Fe	2.393	Ga2:	1	Ru	2.459
	2	Fe	2.500		2	Ru	2.574
	1	Ga2	2.756		1	Ga2	2.832
	2	Ga1	2.835		2	Ga1	2.916
	2	Ga1	2.924		2	Ga1	3.022
	1	Ga2	3.120		1	Ga2	3.165
	1	Ga2	3.351		1	Ga2	3.469
	4	Ga2	3.435		4	Ga2	3.541

Note. SD are all equal to or less than 0.002 Å.

continuously measured, as a potential drop of a generated current, rendering curves with sufficiently small temperature steps. For $RuGa_3$ and $CoGa_3$ the measuring current was $I = 0.1$ mA, while for $FeGa_3$, which had a much higher resistivity, $I = 0.1\,\mu$A and $0.01\,\mu$A were required.

2.4. Electronic Structure Calculations

Total energy calculations for TGa_3 (T = Fe, Ru, Co) were performed within *ab inito* density functional theory as implemented in the program VASP (14). Concerning the pseudopotentials, ultrasoft Vanderbilt-type pseudopotentials (15) were employed considering $(n-1)d$ and ns electrons as valence electrons for T and 3*d*, 4*s*, and 4*p* electrons as valence electrons for Ga. The atomic position parameters and lattice parameters of TGa_3 in the $FeGa_3$ structure type were relaxed for a set of constant volumes until forces had converged to less than 0.01 eV/Å. In a second step we extracted the equilibrium volume V_0 and the ground-state energy E_0 by fitting the E-versus-V values to a Birch–Murnaghan equation of state. The exchange and correlation energy was assessed by the local-density approximation (LDA) (16). Convergence of the calculations was checked with respect to the plane was cutoff and the number of k points used in the summation over the Brillouin zone. Concerning the plane was cutoff an energy value of 300 eV was chosen. K points were generated by the Monkhorst–Pack method (17) and sampled on a $8 \times 8 \times 8$ grid. The integration over the Brillouin zone was performed with the improved tetrahedron method (18).

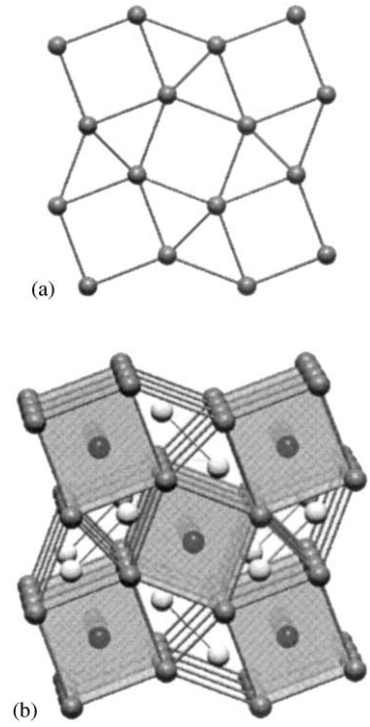

FIG. 1. Description of the tetragonal $FeGa_3$ structure. (a) The 3^2434 net formed by one kind of Ga atoms. (b) Stacking 3^2434 nets on top of each other generates columns of Ga_8 cubes (gray) and Ga_8 rhombic prisms. The cubes are centered by the second kind of Ga atoms; half of the rhombic prisms are occupied by pairs of Fe atoms (white circles).

3. RESULTS AND DISCUSSION

The $FeGa_3$ structure (tetragonal, space group $P4_2/mnm$, $Z = 4$) contains as an important motif, a slightly corrugated 3^2434 net (Fig. 1a), formed by one kind of Ga atoms (Wyckoff site 8*j*). On stacking the 3^2434 nets on top of each other along the *c* direction a tetragonal assembly of columns of (slightly deformed) cubes and rhombic prisms (equivalent to two trigonal prisms sharing a square face) is formed (Fig. 1b). The cubes are centered by the second kind of Ga atoms (Wyckoff site 4*c*), whereas half of the rhombic prisms are occupied by pairs of Fe atoms (Wyckoff site 4*f*). The coordination polyhedron of an Fe atom is an all-square-face capped trigonal prism. In Table 4 we compare the interatomic distances of $FeGa_3$ and $RuGa_3$. Distance in $RuGa_3$ are about 3% longer than those in $FeGa_3$. This scaling can simply be put down to the larger size of Ru compared with Fe which expands the surrounding Ga network. The distances within the pairs of transition metals, 2.77 Å (Fe–Fe) and 2.91 Å (Ru–Ru), indicate only weak interactions, since the nearest-neighbor distances in the respective elemental structures are considerably shorter (2.48 Å (bcc-Fe) and 2.65 Å (hcp-Ru) (19)). Compounds with the $FeGa_3$ structure type are formed exclusively between a transition metal from either the Fe or Co group and one of the element 13 metals Ga and In. The following eight representatives are known: $FeGa_3$, $RuGa_3$, $OsGa_3$, $CoGa_3$, $RuIn_3$, $CoIn_3$, $RhIn_3$, $IrIn_3$ (20–22). Thus, the electron count or valence electron concentration (VEC, number of valence electrons per formula unit) is confined to a range between 17 and 18 electrons. This indicates that compounds with the $FeGa_3$ structure are intermetallic electron compounds (23); i.e., the occurrence of the structure type is governed primarily by the electron count because the band energy term of the total energy determines structural stability.

To investigate in more detail the electronic structure of compounds with the $FeGa_3$ structure we performed first-principle calculations within density functional theory by employing pseudopotentials and a plane wave basis set. We computed the total energy of the systems $FeGa_3$, $RuGa_3$, and $CoGa_3$ which included a complete relaxation of all structural parameters. The results are summarized and compared with the experimental values in Table 5. Apart from the ground-state volume V_0, which typically is obtained around 5% too low within the applied LDA approximation, the agreement between theoretically

TABLE 5
Comparison of the Structural Parameters of TGa_3 (T = Fe, Ru, Co) Obtained from Theory and Experiment

	V_0 (Å^3)	c/a	x_T	x_{Ga}	z_{Ga}
$FeGa_3$					
Theory	239.81	1.045	0.3443	0.1560	0.2631
Exp†[a]	257.09	1.046	0.3437	0.1556	0.2620
$RuGa_3$					
Theory	271.46	1.036	0.3417	0.1554	0.2650
Exp†[a]	280.98	1.036	0.3410	0.1547	0.2640
$CoGa_3$					
Theory	235.23	1.031	0.3461	0.1516	0.2553
Exp†[b]	249.61	1.032	0.3462	0.1520	0.2546

[a]This work.
[b]Reference (13).

modeled and experimentally determined structural parameters is excellent. We now turn to the electronic density of states (DOS) of these three compounds (depicted in Fig. 2) which were calculated at the respective theoretical ground-state volumes. The obtained DOS should represent the electronic structures quite well since the chosen calculational method reproduced perfectly the experimentally obtained structural parameters. First we realize that the DOS curves have a common characteristic overall shape. At low energy the density of states is dominated by approximately parabolically distributed nearly free-electron-like states which stem from the s–p bands of the Ga network and account for the bonding within this network. At higher energy the d states of the transition metal atoms hybridize heavily with the Ga p bands. As a consequence of the $T(d)$–Ga(p) interactions the T d band is split into several parts. If we first focus on $FeGa_3$ we note the part lowest in energy with the largest dispersion of about 2.5 eV (between −3 and −0.5 eV below the Fermi level). This section of the band structure corresponds to strongly d(Fe)–p(Ga) bonded states, whereas the remaining parts with a very narrow dispersion of about 0.5 eV (centered −0.5 and 0.3 eV below and above the Fermi level, respectively) correspond to basically nonbonding states. Importantly, a real bandgap with a size of about 0.3 eV is opened between the two narrow bands at which the Fermi level for $FeGa_3$ is located. The DOS of $RuGa_3$ is similar to that of isoelectronic $FeGa_3$. Since Ru 4d states interact more strongly with Ga p bands than Fe 3d bands, the d–p hybridized bands are broader in $RuGa_3$ and, thus, the two parts lowest in energy have merged. Nevertheless, the bandgap at the Fermi level with a size of about 0.3 eV is maintained. Finally, the band structure of $CoGa_3$ displays perfect rigid band behavior with respect to $FeGa_3$. Since $CoGa_3$ is an 18-electron compound the Fermi level is shifted above the bandgap in $FeGa_3$. It is located in a pseudo gap separating the basically nonbonding states of the second narrow band from antibonding d(T)–p(Ga) states. Summarizing the electronic structure of gallium compounds with the $FeGa_3$ structure, we observe strong interactions between transition metal atoms and Ga atoms that give rise to a bonding–antibonding splitting of $d(T)$–p(Ga) hybridized states and the opening of a bandgap at the Fermi level for 17-electron compounds. This corresponds exactly to the situation encountered for the AB_2 compounds $RuAl_2$ and $RuGa_2$ with the $TiSi_2$ structure where the bandgap coincides with the Fermi level in the case of 14-electron compounds (5). Thus, we understand easily the dominating role of VEC for the stability of the $FeGa_3$ structure type: an electron count of 17 corresponds to the filling of all bonding states and a VEC of 18, additionally to the filling of all nonbonding ones. The peculiar electronic structure of compounds with the $FeGa_3$ structure should also be reflected in their transport properties.

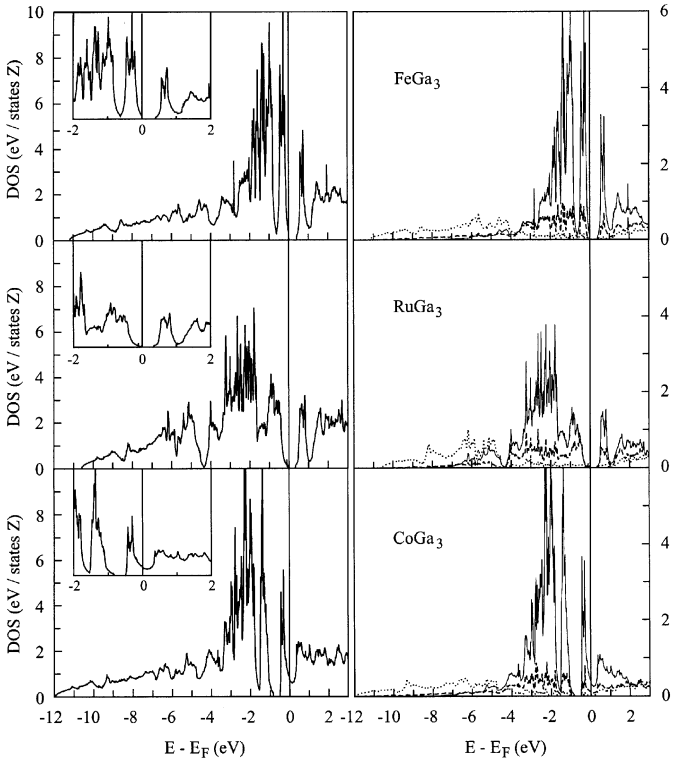

FIG. 2. Left: Total density of states (DOS) for the compounds $FeGa_3$, $RuGa_3$ and $CoGa_3$. Insets: Closeups of the DOS for the states around the Fermi level. Right: Decomposition of the DOS into transition metal d (solid line), Ga-s (dotted line), and Ga-p (broken line) states.

The resistivity ρ of $FeGa_3$, $RuGa_3$ and $CoGa_3$ is shown in Fig. 3. As expected from the theoretical investigations the resistivity of $FeGa_3$ and $RuGa_3$ is clearly semiconducting (ρ decreases with increasing temperature), whereas for $CoGa_3$ ρ increases linearly with increasing temperature typical of metallic conductors. Thus, on a qualitative basis the resistivity measurements reflect the electronic structure

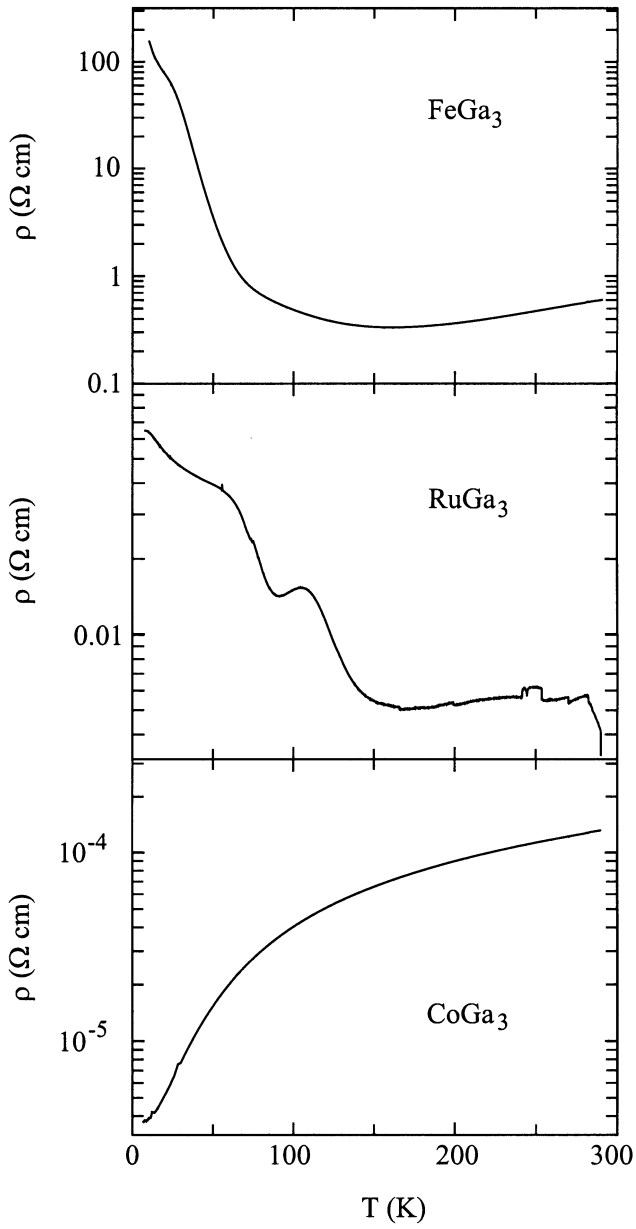

FIG. 3. Resistivity as a function of temperature (logarithmic scale) of $FeGa_3$, $RuGa_3$, and $CoGa_3$.

of these compounds obtained from first-principle calculations. However, the detailed temperature dependence of ρ for $FeGa_3$ and $RuGa_3$ is much more complicated and not completely understood by us. Although ρ clearly decreases with increasing temperature neither curve displays linearity between $\log(\rho)$ and $1/T$. Focusing first on $FeGa_3$ we observe a large decrease in ρ of more than two orders of magnitude in the small temperature range from 10 to 60 K. This indicates a very small bandgap, at least one order of magnitude smaller than the calculated one. The resistivity attains a minimum at about 160 K ($\approx 0.325\,\Omega$ cm) after which it increases to a value of 0.6 Ω cm at room temperature. Such high resistivity values, however, are rather incompatible with a very small bandgap. For comparison, elemental Te with a bandgap of 0.33 eV has a room temperature resistivity of about 0.65 Ω cm (24), which is very similar to that of $FeGa_3$. Additionally, it appears to be unlikely that the calculated bandgap should be underestimated by at least one order of magnitude since the structural parameters are so well reproduced by the chosen calculational method and further the LDA approximation is actually known to underestimate bandgaps. The behavior of $RuGa_3$ is similar to that of $FeGa_3$ apart from the occurrence of a kink at about 100 K and the "jagged" part above 250 K, which most likely is due to contact problems. The resistivity of $RuGa_3$ in the temperature range 150 to 250 K (and probably up to room temperature) is two orders of magnitude lower than that of $FeGa_3$ and would be comparable to that of main-group narrow-bandgap semiconductors, like InSb (24). The occurrence of a minimum in the ρ-versus-T curves for both compounds remind us of the exhaustion behavior of doped semiconductors. Exhaustion is the temperature range with an almost constant concentration of charge carriers in which low-temperature extrinsic conductivity changes to high-temperature intrinsic conductivity. Thus it might be quite possible that the conductivity of our investigated crystals $FeGa_3$ and $RuGa_3$ up to room temperature is of (complicated) extrinsic nature arising from defects or small amounts of impurities. To extract bandgaps mirroring the ones in the calculated density of states the temperature dependence of the intrinsic conductivity (at higher temperatures) has to be measured. This and also the explicit dependency of resistivity on crystal lattice directions will be the subject of further investigations.

In conclusion we find that 17-electron compounds with the $FeGa_3$ structure should exhibit semiconductivity because the Fermi level is located at a bandgap in the electronic density of states. This suggests that $OsGa_3$ and $RuIn_3$ are semiconductors as well. To our knowledge, for $OsGa_3$ no resistivity data are reported. $RuIn_3$, however, was found to be a poor metallic conductor with a high room temperature value of about 0.0038 Ω cm (i.e., the same order of magnitude as that of $RuGa_3$) (21). This can be explained by the fact that T–In interactions are considerably weaker than T–Ga interactions (25). Thus, $d(T)$–p(In) hybridization in $RuIn_3$ produces just a pseudo gap (with a low value of the DOS at the Fermi level) instead of a real bandgap as the gallium compounds.

4. CONCLUSIONS

$FeGa_3$ and $RuGa_3$ were found to be semiconducting, which is an unusual property for compounds formed exclusively by elemental metals with good conductivity.

Hitherto $RuAl_2$ and $RuGa_2$ were the only known "true" intermetallic (narrow-bandgap) semiconductors. The origin of the semiconducting behavior of those compounds is strong directional (covalent) interactions between transition metal atoms and *p*-block atoms which result in a bonding–antibonding splitting of *d*(*T*)–*p*(Ga) hybridized states and the opening of a bandgap at the Fermi level. It is interesting to speculate if there are more examples of such *d*–*p* bonded intermetallic semiconductors. If one defines intermetallic compounds restrictively to compounds between metallic conducting elements the only possible *p*-block elements seem to be Al and Ga because *p*-block elements from the higher rows in the periodic table (e.g., In, Sn) interact considerably more weakly with transition metals (25). Second, the choice of transition metal seems to be limited to those from the middle of each series because for these elements the energy of the atomic *d* states matches approximately the Fermi level of the *s*–*p* bonded network of *p*-block atoms. This situation gives the most effective interaction between both components (26). Third, there are restrictions on the crystal structure and composition as well. To ensure maximum *d*–*p* bonding the composition can neither be too rich in the transition metal component nor too rich in the *p*-block component. In the case of the former direct (*d*–*d*) interactions between transition metal atoms will lead to broadening of the *d*-based bands and eventually to closure of the bandgap. In the case of the latter the concentration of transition metal atoms will be too low to effectively remove the *s*–*p*-based bands of the network of *p*-block atoms from the Fermi level. Thus, with this manifold of restrictions it appears to be difficult to find further examples of semiconducting "true" intermetallic compounds. Apart from $OsGa_3$ with the $FeGa_3$ structure from theoretical investigations we also identified $OsAl_2$ with the $MoSi_2$ structure (27) as a potential semiconductor (calculated bandgap of 0.2 eV) (26).

ACKNOWLEDGMENTS

This work was supported by the Swedish National Science Research Council (NFR) and the Göran Gustafsson Foundation.

REFERENCES

1. F. S. Pierce, S. J. Poon, and B. D. Biggs, *Phys. Rev. Lett.* **70,** 3919 (1993).
2. D. Mandrus, V. Keppens, B. C. Sales, and J. L. Sarrao, *Phys. Rev. B* **58,** 3712 (1998).
3. J. Evers, G. Oehlinger, and H. Meyer, *Mater. Res. Bull.* **19,** 1177 (1984).
4. W. Jeitschko, *Acta Crystallogr. Sect. B* **33,** 2347 (1977).
5. D. Nguyen Manh, G. Trambly de Laissardière, J. P. Julien, D. Mayou, and F. Cyrot-Lackmann, *Solid State Commun.* **82,** 329 (1992).
6. P.-E. Werner, *Ark. Kem.* **31,** 513 (1969).
7. S. S. Lu and Liang Ching-Kwei, *Chin. Phys.* **212,** 1079 (1959).
8. K. Schubert, H. L. Lukas, H.-G. Meissner, and S. Bhan, *Z. Metallkd.* **50,** 534 (1959).
9. "SMART Reference Manual." Siemens Analytical X-ray Instruments Inc., Madison, WI, 1996.
10. "ASTRO and SAINT: Data Collection and Processing Software for the SMART System." Siemens Analytical X-ray Instruments Inc., Madison, WI, 1995.
11. G. M. Sheldrick, "SADABS, Program for Scaling and Correction of Area Detector Data." Univ. of Göttingen, Germany, 1996.
12. G. M. Sheldrick, "SHELXTL," Version 5.1, Bruker AXS, Madison, WI, 1998.
13. P. Viklund, S. Lidin, P. Berastegui, and U. Häussermann, *J. Solid State Chem.* **164,** 100 (2002).
14. (a) G. Kresse and J. Hafner, *Phys. Rev. B* **47,** RC558 (1993); (b) G. Kresse and J. Furthmüller, *Phys. Rev. B* **54,** 11169 (1996).
15. (a) D. Vanderbilt, *Phys. Rev. B* **41,** 7892 (1990); (b) G. Kresse and J. Hafner, *J. Phys. Condens. Matter* **6,** 8245 (1994).
16. J. Perdew and A. Zunger, *Phys. Rev. B* **23,** 5048 (1981).
17. H. J. Monkhurst and J. D. Pack, *Phys. Rev. B* **13,** 5188 (1976).
18. P. Blöchl, O. Jepsen, and O. K. Andersen, *Phys. Rev. B* **49,** 16223 (1994).
19. T. S. Massalski, "Binary Alloy Phase Diagrams," 2nd ed. Am. Soc. for Metals, Metals Park, OH, 1990.
20. P. Villars and L. D. Calvert, "Pearsons Handbook of Crystallographic Data for Intermetallic Phases," 2nd ed. Am. Soc. for Metals, Materials Park, OH, 1991; desk ed., 1997.
21. R. Pöttgen, *J. Alloys. Compd.* **226,** 59 (1995).
22. R. Pöttgen, R.-D. Hoffmann, and G. Kotzyba, *Z. Anorg. Allg. Chem.* **624,** 255 (1998).
23. R. Ferro and A. Saccone, *in* "Materials Science and Technology" (R. W. Cahn, P. Haasen, and E. J. Kramer, Eds.), Vol. 1: The Structure of Solids. VCH, Weinheim, 1993.
24. O. Madelung, M. Schultz, and H. Weiss (Eds.), "Landolt–Börnstein, New Series," Vol. 17: Semiconductivity. Springer-Verlag, Berlin, 1982.
25. U. Häussermann, P. Viklund, M. Boström, R. Norrestam, and S. I. Simak, *Phys. Rev. B* **63,** 125118 (2001).
26. U. Häussermann, unpublished results.
27. L.-E. Edshammar, *Acta Chem. Scand.* **19,** 871 (1965).